

# DERIVING SUN-INDUCED CHLOROPHYLL FLUORESCENCE FROM AIRBORNE BASED SPECTROMETER DATA

Alexander Damm<sup>(1)</sup>, Anke Schickling<sup>(2)</sup>, Daniel Schläpfer<sup>(1)</sup>, Michael Schaepman<sup>(1)</sup>, and Uwe Rascher<sup>(2)</sup>

<sup>(1)</sup> Remote Sensing Laboratories, University of Zurich – Irchel, Winterthurerstrasse 190, CH-8057, Zürich, (Alexander.Damm, Daniel.Schlaepfer, Michael.Schaepman)@geo.uzh.ch

<sup>(2)</sup> Institute of Chemistry and Dynamics of the Geosphere, ICG-3: Phytosphere, Forschungszentrum Jülich, Stettericher Forst, 52425 Jülich, Germany, (a.schickling, u.rascher)@fz-juelich.de

## ABSTRACT

Sun-induced chlorophyll fluorescence (Fs) is a promising parameter for remote measuring plant photosynthesis. It has been demonstrated that Fs at cell and leaf level is strongly related to photosynthesis. The transfer of the Fs approach to canopy level remains challenging as the canopy Fs signal is not fully understood yet. Several factors influence the Fs signal and need to be quantified. However, the absence of dedicated imaging spectrometers limits the experimental data for such investigations. We propose an experimental setup allowing spatio-temporal investigations of canopy Fs. A non-imaging spectrometer was installed in a low-flying aircraft. An agricultural area was continuously monitored including the extensive coverage of dedicated fields. Fs was retrieved from spectrometer data using the FLD (Fraunhofer Line Depth) method combined with simulated (MODTRAN-4) at-sensor radiances of a reference surface. We present the methodological framework to derive canopy chlorophyll fluorescence from airborne based non-imaging spectrometer measurements and a quality assessment of the data.

## 1. INTRODUCTION

Photosynthesis is a key process in terrestrial ecosystems, mediating 90% of carbon and water fluxes (Ozanne et al. 2003). Slight alterations of terrestrial carbon balance significantly influence atmospheric carbon dioxide (CO<sub>2</sub>) concentrations. Exact quantifications and improved understanding of this interrelationship are essential for a sustainable use of natural resources or an adequate exposure with consequences from the newest IPCC report (IPCC 2008).

Much effort in bio-geoscience research has been put in improving the understanding of CO<sub>2</sub> fluxes at different temporal and spatial scales (Baldocchi 2003; Cohen et al. 2003; Turner et al. 2003). For quantifying current fluxes, an extensive network of eddy covariance (EC) towers was established during the past decades. The well established eddy covariance (EC) technique provides local but temporally high resolved flux measurements of the underlying ecosystem. However, monitoring and quantification of the spatio-temporal

dynamic of carbon fluxes is essential. Remote sensing provides the unique possibility for spatial explicit estimates of current photosynthetic rates. Thereby, sun-induced chlorophyll fluorescence seems promising to track actual photosynthetic activity. Extensive work has been carried out at cell and leaf level clearly demonstrating that Fs is strongly related to photosynthesis. In consequence, recent activities suggest that the remote measurable Fs can serve as proxy for photosynthesis. Advances in sensor technology nowadays allow remote observations of the emitted fluorescence signal at leaf scale with reliable accuracy. Results from several studies indicate that chlorophyll fluorescence also track changes of photosynthetic rates at small canopy level (Damm et al. 2010).

A couple of influencing factors were identified which superimpose the variability of Fs induced by changing photosynthetic rates. Absorption processes within the atmosphere, environmental conditions, structural canopy properties, and technical effects strongly influence the optical measured Fs signal (Meroni et al. 2009). These effects must be quantified and corrected to provide comparable Fs estimates as proxy for photosynthesis. Currently, only a few imaging sensors (e.g. CASI-1500) (Alonso et al. 2008; Guanter et al. 2007) exists, which are capable to provide reliable and spatial explicit maps of Fs. Hence, the experimental base of dedicated observation is strongly limited.

Objective of our work was to establish an experimental setup for a spatial explicit observation of canopy Fs. A non-imaging ASD spectrometer was installed in a DIMONA aircraft flying at low altitude. Data were subsequently corrected for platform movements and Fs was retrieved from spectrometer data using the FLD (Fraunhofer Line Depth) method in combination with an atmospheric radiative transfer model (MODTRAN-4). The experiment took place in an extended agricultural test site and explicitly includes dedicated validation measurements. Individual winter wheat and sugar beet fields were extensively covered in the course of a day by in-situ small canopy scale Fs measurements and airborne based canopy measurements. While keeping the instrumented approach the same, an evaluation of the Fs signal quality was possible.

We present the methodological framework for deriving chlorophyll fluorescence from airborne based non-imaging spectrometer measurements and results from the data analysis. This includes the validation of airborne based  $F_s$  estimates against temporal ground observations performed simultaneously with the overflights.

## 2. DATA AND METHODS

### 2.1. Data

Used datasets basically consist of extended transects of airborne based non-imaging spectrometer measurements and three diurnal courses of ground based spectrometer data (Table 1). Data acquisition took place within the FLUXPAT field campaign in 2008 near Cologne, Germany.

Table 1: Overview of acquired data

Date in 2008	time DIMONA (UTC)	time ASD (UTC)	weather condition	canopy
23.04.	08:30-12:30	8:30-13:00	clear	winter wheat
24.06.	11:20-15:30	7:30-16:00	clear	winter wheat
01.07.	07:30-10:30 11:15-16:00	7:00-16:00	clear	sugar beet

#### *DIMONA overflights*

A small low-flying research aircraft (Metair AG, Switzerland) was used as platform for the non-imaging spectrometer ASD FieldSpec Pro II (Analytical Spectral Devices, Boulder, USA). The spectrometer was mounted in the lefthand underwing pod. Radiation reflected from the Earth surface was captured in nadir orientation with a 1 degree fiber optic. The incident radiation was measured in the spectral range from 350 to 1050 nm, with a FWHM of 3.0 nm and a spectral sampling interval of 1.4 nm. The instrument was operated in continuous mode and spectra were collected with approximately 2 Hz. Integration time of the ASD was adjusted to 136 ms for best signal to noise ratio and to avoid saturation. Three single spectra were averaged and saved to improve data quality (Eiden et al. 2007). A magnitude of auxiliary data was recorded to support subsequent data pre-processing. This includes atmospheric parameters ( $CO_2$ ,  $H_2O$ ,  $CO$ ,  $NO_x$ ) (Neininger 2001; Schmitgen et al. 2004) and flight positioning data using a TANS Vector phase sensitive GPS system blended with 3-axis accelerometers. Data pre-processing consist of a platform movement correction and the geo-location of each measurement. The correction of atmospheric effects was integral part of the retrieval algorithm itself (see next section).



Figure 1: Flight patterns of one Dimona overflight on the 1<sup>st</sup> July 2008 near Cologne.

#### *ASD ground data*

An ASD FieldSpec Pro III spectroradiometer was used to acquire diurnal courses of reflected radiation from dedicated fields of interest. A calibrated Spectralon<sup>TM</sup> panel (25×25 cm) served as white reference to estimate incident irradiance. The instrument's fibre optic was mounted on a robotic arm of 0.6m length, approximately 1m above the canopy. The movement of the robotic arm allowed to automatically collecting daily cycles of four different canopy spots with a circular area of about 0.5m diameter each. The acquired dataset consists of spectral records from four canopy areas, bracketed by measurements of the reference panel. Integration time was automatically optimized during the day in order to maximize the instrument signal to noise ratio.

#### *MODTRAN simulations*

The radiative transfer model MODTRAN-4 (MODerate spectral resolution atmospheric TRANsmittance algorithm) (Berk et al. 1999a; Berk et al. 1999b) was used to simulate the reflected radiation of a Spectralon<sup>TM</sup> reference panel at sensor level. The simulated radiance signals are needed as reference signal for retrieving  $F_s$  and for calculating reflectance factor values. The later one is the base for a series of spectral vegetation indices characterizing the vegetation in biochemical and structural terms.

MODTRAN4 was parameterized with realistic atmospheric properties (Table 2). A look-up-table (LUT) was calculated containing individual simulations to account for changing flight heights and observation times of the DIMONA overflights. Therefore, the sensor altitude and both sun-zenith and sun-azimuth angle were systematically varied. The height interval was adjusted to 10 m and the time interval to 1 h. The simulations of the resulting LUT were subsequently spline-interpolated to provide a height resolution of 1 m and a time resolution of 1 second.

Table2: MODTRAN4 parameters for the 1<sup>st</sup> July 2008

Parameter	Unit	Value
Correlated-K option	-	yes
DISORT number of streams	-	8
Molecular band model resolution	cm <sup>-1</sup>	1
Profile	-	midlatitude summer
Aerosol model	-	urban ext. V23
Visibility	km	50
Surface height	km	0.06
Sensor height	km	0.001-0.5
Water vapour	g cm <sup>-2</sup>	1.3
CO <sub>2</sub>	ppm	365
Solar azimuth angle	deg	45.3-311.5
Solar zenith angle	deg	94-27.6-92
Viewing zenith angle	deg	180

All simulated at-sensor radiance signals were convolved (FWHM 3.0 nm) and sampled (sampling interval 1.4 nm) considering the sensor properties of the ASD spectrometer. The previously estimated spectral miss-registration was considered during the re-sampling process. Afterwards, a cubic convolution was applied to provide 1nm resolution. This was necessary as the ASD spectrometer interpolates the response of a particular channel to a value at 1 nm wavelength spacing, basically using a cubic spline interpolation (ASD, personal communication).

## 2.2 Methods

### FLD

F<sub>s</sub> adds a weak signal to the reflected solar radiation of the vegetated canopy. The emitted F<sub>s</sub> is characterized by a well defined spectral shape and two broad peaks at about 685 and 740 nm (Franck et al. 2002; Lichtenthaler and Rinderle 1988). However, the amount of emitted F<sub>s</sub> is only about 1-5% of the total reflected light (near-infrared) at a certain wavelength. This low magnitude makes the separation of both fluxes to a challenging problem. The Fraunhofer Line Depth (FLD) principle, introduced by (Plascyk 1975), is currently one of the most often used approaches to retrieve F<sub>s</sub> from radiometric measurements. The method was successfully used in different works (Carter et al. 1990; Damm et al. 2010; Moya et al. 2004). The FLD principle assumes that F<sub>s</sub> is additive to the reflected signal and can be derived by comparing the depth of the O<sub>2</sub> absorption band from a non-fluorescent surface (W) with that of the vegetation target (V). In this study, we applied a modified version of the original FLD principle (Maier et al. 2003) on the O<sub>2</sub>-A band. The method is a continuum interpolated band ratio (CIBR), using two reference channels on both sides of an absorption band to estimate the band depth for both, the non-vegetated and the vegetated surface. The reference channel is calculated as interpolated value between two channels outside of the band (755 and 772 nm) at the wavelength position of the absorption band (760.6 nm). The band depth is the ratio between the interpolated reference channel (V2, W2) and the band value (V1, W1). The

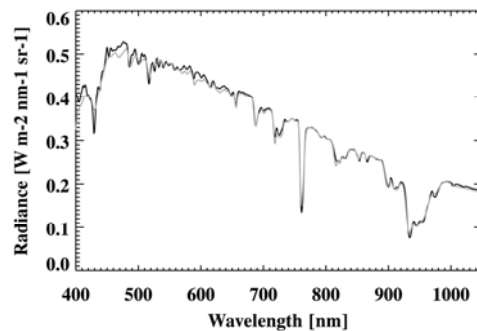
additive F<sub>s</sub> signal is derived as normalized difference between observed band value of the vegetated surface (V1) and the modelled one (equation 1).

$$F_s = \frac{V_1 - \frac{W_1}{W_2} \cdot V_2}{1 - \frac{W_1}{W_2}} \quad (1)$$

The reference signals which are un-perturbed from fluorescence emission were simulated with MODTRAN-4 and stored in a LUT. Each spectrometer measurement onboard the DIMONA aircraft was taken together with a measurement of the actual flight height and observation time. Both auxiliary parameters were used to select representative simulations from the MODTRAN-LUT.

## 3. RESULTS AND DISCUSSION

The plausibility of MODTRAN simulated at-sensor radiances was proofed by comparing the ground based Spectralon<sup>TM</sup> measurements and the simulated signals. Figure 2-top and 2-bottom shows the agreement between both signals in radiance units. Obvious miss-agreements occur near strong absorption features and appear as spikes in the calculated reflectance factor signals. These errors may be induced by i) non-uniform spectral miss-alignments of the sensor, ii) variable FWHM and spectral sampling interval characterizations, or iii) a shift of the spectral band position of absorption features induced by an insufficient description of the atmosphere. Empirical calibration factors were derived for reducing the impact of these errors in subsequent analyses. Both radiance signals of a corresponding observation time and sensor height were divided. The resulting factors were applied to all modelled reference radiances of the same time but variable sensor heights.



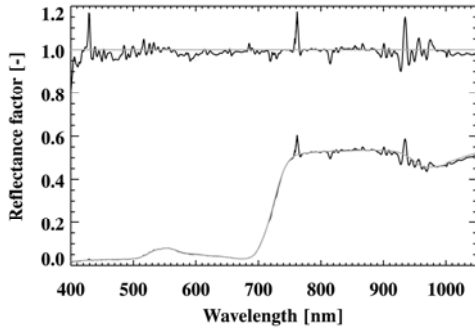


Figure 2: Modelled and measured signals. Top: Radiance signals of a Spectralon<sup>TM</sup> panel (grey: measured and empirical corrected, black: modelled). Bottom: Reflectance factor values of a Spectralon<sup>TM</sup> panel and a vegetation surface. The grey reflectance factor values are calculated using a measured white-reference, the black reflectance factor values are based on a modelled white reference.

#### MODTRAN4 sensitivity analysis

The air mass between sensor and surface modifies the signal reflected from the surface due to molecular absorption effects and aerosol scattering. The path length between surface and sensor as consequence of flight height and sun position was highly variable during the data acquisition. Two sensitivity analyses were performed to quantify the theoretical impact of both effects on the O<sub>2</sub>-A band depth received by the sensor. A first analysis was dedicated to quantify the impact of sensor height on the O<sub>2</sub>-A band depth and related radiance signals (Figure 3). Both radiance signals (755 and 760.0 nm) non-equally decrease with an increasing distance from surface-sensor for the bright Spectralon<sup>TM</sup> panel due to the decreasing transmittance. The O<sub>2</sub>-A band depth non-linearly increases from 6.27 to 6.97 considering a flight height range of 450 m (50-500 m). This behaviour seems plausible as the concentration of atmospheric oxygen exponentially decrease with increasing height above ground.

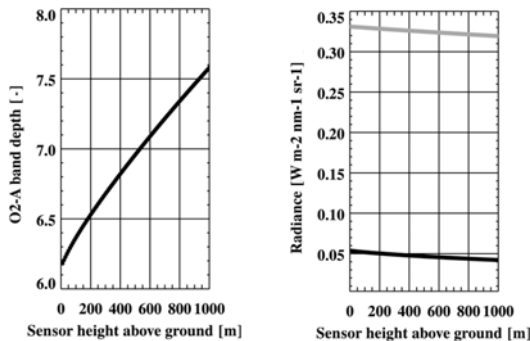


Figure 3: Dependency of O<sub>2</sub>-A band depth (left), the radiance signal outside (755 nm) (grey) and inside

(760.6 nm) (black) of the absorption band (right) on flight height.

A second analysis was quantifying the impact of the sun-position on the O<sub>2</sub>-A band depth and underlying radiance signals (Figure 4). The sun position was parameterized with the sun-azimuth and the sun-zenith angle for a certain time of the day.

The radiance signals used to obtain the band depth (755 and 760.6 nm) show a typical symmetric behaviour with increasing radiance until noon and a decrease in the afternoon hours. The O<sub>2</sub>-A band depth non-linearly decreases in the morning, reaches a minimum at solar noon and increases in the afternoon. The observed behaviour is plausible and can be explained with a change in the path length of the irradiance and the location of the pathway with respect to the Earth surface. Assuming a homogeneous atmospheric O<sub>2</sub>-concentration, the amount of absorbed radiance due to O<sub>2</sub> is linear related to the path length. This relationship is superimposed by the exponential increase of atmospheric O<sub>2</sub>-concentrations with decreasing distance to the Earth surface. The variation of the O<sub>2</sub>-A band depth with respect to the time of over-flight (10:00-17:30) is about 2.87 (Figure 4).

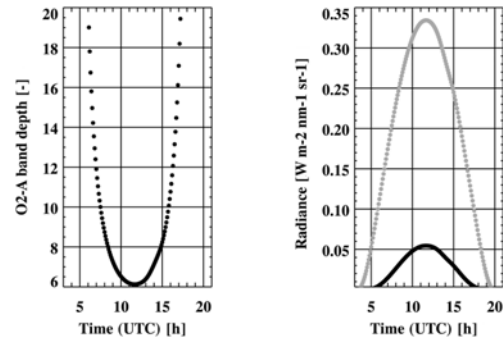


Figure 4: Dependency of O<sub>2</sub>-A band depth (left), the radiance signal outside (755 nm) (grey) and inside (760.6 nm) (black) of the absorption band (right) on sun position (zenith and azimuth)

#### Quality assessment of airborne based canopy Fs

The diurnal course of ground based Fs measurements continuously increases in the morning hours, reaches a maximum around solar noon and decreases in the afternoon (Figure 5). This behaviour was expected as the fluorescence emission is directly related to the amount of incident light.

The Fs signals derived from airborne measurements principally follow the same diurnal course. However, the Fs signals are lower with respect to the ground measurements and show a certain amount of variation. The underestimation (scaling factor 0.3) seems plausible: The emitted fluorescence signal is re-absorbed on the way from the surface to the sensor.

Whether the scaling factor is in the correct order of magnitude needs to be investigated.

The scattering of the diurnal course can be attributed to the fact that different canopy areas of the entire field were covered during the day. Another source of variability was induced by changing flight heights, which vary the size of the measured canopy area.

Both curves deviate in their temporal pattern. Most obvious is the underestimation of the airborne signal in the morning. This miss-agreement may be attributed to two effects: i) Leaves of the observed sugar-beet plants are characterized by a waxy cuticle and plants were seeded in rows. In consequence, the canopy is affected by strong bi-directional effects. Both the airborne and the ground setup were covering different parts of the canopy at different scales. These differences change the impact of bi-directional effects on the measured signals. ii) The used LUT does not account for changing aerosol and water vapour concentrations. However, both atmospheric properties significantly vary the amount of re-absorption of the Fs signal on the way from the surface to the sensor.

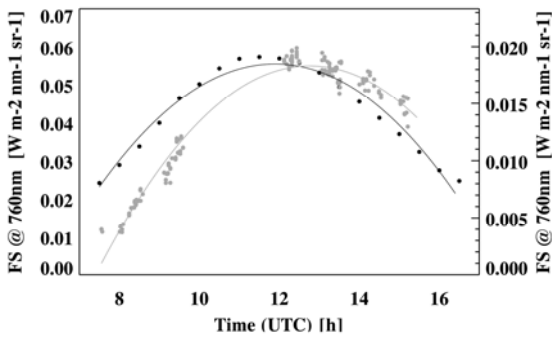


Figure 5: Comparison of ground based (black, 1<sup>st</sup> y-axis) and airborne based Fs (grey, 2<sup>nd</sup> y-axis) during the course of the 1<sup>st</sup> July 2008. Two second degree polynomial fits are overlaid.

The comparison of both curves indicates the reliability of airborne based Fs observations in the course of a day. A further investigation should give some indications whether the spatial variability of Fs signals are realistic or not. Figure 6 presents a comparison between the well established Normalized Difference Vegetation Index (NDVI) and canopy Fs.

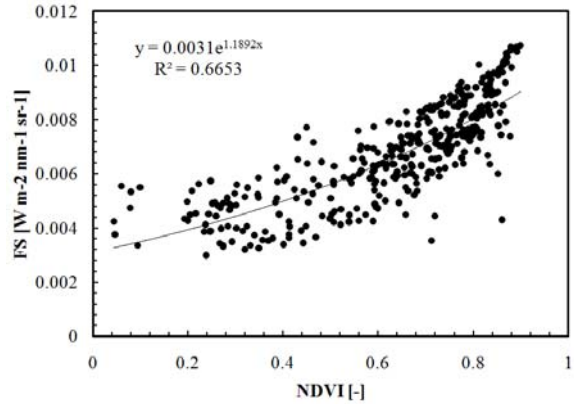


Figure 6: Comparison between the vegetation index NDVI and canopy Fs. Both parameters are obtained from airborne based spectrometer data.

The graph shows a strongly scattered, non-linear relationship between both variables. The NDVI represents the “greenness” of a vegetation canopy i.e. the index is a measure for green biomass or canopy chlorophyll content (Goetz and Prince 1999). Fluorescence is a function of canopy chlorophyll content. Hence, low Fs values should correspond to low NDVI values and vice versa. The scattering and non-linearity may be explained by the theoretically dependency of the NDVI to photosynthetic pigments, whereas Fs covers complementary information about the activity of the photosynthetic apparatus.

#### 4. CONCLUSIONS

Several external factors superimpose remotely measured canopy Fs signals. A quantification of these effects is essential to allow a proper correction and, in consequence, to provide comparable Fs values. Due to the absence of dedicated imaging spectrometers, we proposed an experimental setup allowing spatial explicit and temporally flexible measurements of canopy Fs.

A combination of airborne based ASD measurements combined with modelled at-sensor radiances of a reference surface was established to measure canopy Fs. Our results indicate that the proposed approach provides reliable Fs measurements.

Special attention must be paid on an accurate description of the sensor characteristics, e.g. spectral calibration. Spectral miss-registration leads to incorrect absolute Fs measurements.

The LUT containing at-sensor irradiance spectra must account for variable sun positions and flight heights. Furthermore, our results indicate that the LUT should consider changing aerosol concentrations to account for the re-absorption of the emitted Fs signal.

An empirical correction of the LUT using in-situ radiometric measurements is suggested. This mainly compensates incorrect atmospheric descriptions and potential sensor miss-calibrations.

## REFERENCES

- Alonso, L., Gómez-Chova, L., Vila-Francés, J., Amorós-López, J., Guanter, L., Calpe, J., & Moreno, J. (2008). Improved Fraunhofer Line Discrimination method for vegetation fluorescence quantification. *Ieee Geoscience and Remote Sensing Letters*, *5*, 620-624
- Baldocchi, D.D. (2003). Assessing the eddy covariance technique for evaluating carbon dioxide exchange rates of ecosystems: past, present and future. *Global Change Biology*, *9*, 479-492
- Berk, A., Anderson, G.P., Bernstein, L.S., Acharya, P.K., Dothe, H., Matthew, M.W., Adler-Golden, S.M., J.H. Chetwynd, J., Richtsmeier, S.C., Pukall, B., Allred, C.L., Jeong, L.S., Hoke, M.L., & Green, R. (1999a). MODTRAN4 Radiative Transfer Modeling for Atmospheric Correction. In, *8th Ann. JPL Airb. Earth Science Workshop* (pp. 55-61)
- Berk, A., Anderson, G.P., Acharya, P.K., Chetwynd, J.H., Bernstein, L.S., Shettle, E.P., Matthew, M.W., & Adler-Golden, S.M. (1999b). MODTRAN4 Version 3 Revision 1 User's Manual. In, *AIR FORCE RESEARCH LABORATORY Space Vehicles Directorate, Hanscom AFB, MA 01731-3010* (p. pp. 101)
- Carter, G.A., Theisen, A.F., & Mitchell, R.J. (1990). Chlorophyll fluorescence measured using the Fraunhofer Line-Depth principle and relationship to photosynthetic rate in the field. *Plant Cell and Environment*, *13*, 79-83
- Cohen, W.B., T.K., M., & Yang, Z.Q. (2003). Comparisons of land cover and LAI estimates derived from ETM plus and MODIS for four sites in North America: a quality assessment of 2000/2001 provisional MODIS products *Remote Sensing of Environment*, *88*, 256-270
- Damm, A., Erler, A., Gioli, B., Hamdi, K., Hutjes, R., Kosvancova, M., Meroni, M., Miglietta, F., Moersch, A., Moreno, J., Schickling, A., Sonnenschein, R., Udelhoven, T., Van der Linden, S., Hostert, P., & Rascher, U. (2010). Remote sensing of sun induced fluorescence yield to improve modelling of diurnal courses of Gross Primary Production (GPP). *Global Change Biology*, *16*, 171-186
- Eiden, M., van der Linden, S., Schween, J., Gerbig, C., Neininger, B., Traulle, O., Geiss, H., & Rascher, U. (2007). Elucidating the interaction of plants in the carbon dioxide cycle using airborne hyperspectral reflectance measurements in synopsis with eddy covariance data. In, *10th ISPMSRS*. Davos, Switzerland
- Franck, F., Juneau, P., & Popovic, R. (2002). Resolution of the Photosystem I and Photosystem II contributions to chlorophyll fluorescence of intact leaves at room temperature. *Biochimica Et Biophysica Acta-Bioenergetics*, *1556*, 239-246
- Goetz, S.J., & Prince, S.D. (1999). Modelling terrestrial carbon exchange and storage: Evidence and implications of functional convergence in light-use efficiency. *Advances in Ecological Research*, *Vol 28* (pp. 57-92)
- Guanter, L., Alonso, L., Gomez-Chova, L., Amoros-Lopez, J., Vila, J., & Moreno, J. (2007). Estimation of solar-induced vegetation fluorescence from space measurements. *Geophysical Research Letters*, *34*, doi: 10.1029/2007GL029289
- IPCC (2008). Climate Change 2007: Synthesis report. In
- Lichtenthaler, H.K., & Rinderle, U. (1988). The role of chlorophyll fluorescence in the detection of stress conditions in plants. *Crc Critical Reviews in Analytical Chemistry*, *19*, S29-S85
- Maier, S.W., Günther, K.P., & Stellmes, M. (2003). Sun-Induced Fluorescence: A New Tool for Precision Farming. In M. McDonald, J. Schepers, L. Tartly, T. van Toai & D. Major (Eds.), *Digital Imaging and Spectral Techniques: Applications to Precision Agriculture and Crop Physiology* (pp. 209-222): ASA Special Publication
- Meroni, M., Rossini, M., Guanter, L., Alonso, L., Rascher, U., Colombo, R., & Moreno, J. (2009). Remote sensing of solar induced chlorophyll fluorescence: review of methods and applications. *Remote Sensing of Environment*, doi:10.1016/j.rse.2009.05.003
- Moya, I., Camenen, L., Evain, S., Goulas, Y., Cerovic, Z.G., Latouche, G., Flexas, J., & Ounis, A. (2004). A new instrument for passive remote sensing 1. Measurements of sunlight-induced chlorophyll fluorescence. *Remote Sensing of Environment*, *91*, 186-197
- Neininger, B. (2001). A small aircraft for more than just ozone: Metair's "Dimona" after ten years of evolving development. In, *11th Symposium on Meteorological Observations and Instrumentation, 81st AMS Annual Meeting*. Albuquerque, NM, USA
- Ozanne, C.M.P., Anhof, D., Boulter, S.L., Keller, M., Kitching, R.L., Komer, C., Meinzer, F.C., Mitchell, A.W., Nakashizuka, T., Dias, P.L.S., Stork, N.E., Wright, S.J., & Yoshimura, M. (2003). Biodiversity meets the atmosphere: A global view of forest canopies. *Science*, *301*, 183-186

- Plascyk, J.A. (1975). MK II Fraunhofer Line Discriminator (FLD-II) for airborne and orbital remote-sensing of solar-stimulated luminescence. *Optical Engineering*, 14, 339-346
- Schmitgen, S., Geiss, H., Ciais, P., Neininger, B., Brunet, Y., Reichstein, M., Kley, D., & Volz-Thomas, A. (2004). Carbon dioxide uptake of a forested region in southwest France derived from airborne CO<sub>2</sub> and CO measurements in a quasi-Lagrangian experiment. *Journal of Geophysical Research-Atmospheres*, 109
- Turner, D.P., Ritts, W.D., Cohen, W.B., Gower, S.T., Zhao, M.S., Running, S.W., Wofsy, S.C., Urbanski, S., Dunn, A.L., & Munger, J.W. (2003). Scaling Gross Primary Production (GPP) over boreal and deciduous forest landscapes in support of MODIS GPP product validation. *Remote Sensing of Environment*, 88, 256-270